AD-A032 046 NAVAL RESEARCH LAB WASHINGTON D C F/G 20/14
NUMERICAL SOLUTION OF THE PARABOLIC EQUATION WITH THE PEP CODE.(U)
OCT 76 B E MCDONALD

UNCLASSIFIED NRL-MR-3385 NL

1 OF 1
ADA032046

END

DATE
FILMED
1 -77

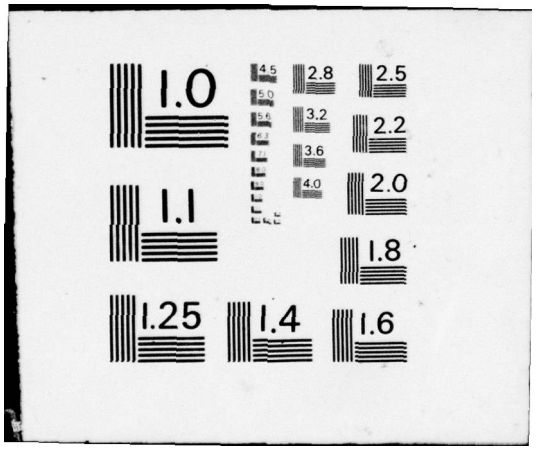
1.0
1.1
1.25
1.4
1.6
1.8
2.0
2.2
2.5
2.8
3.2
3.6
4.0
4.5
5.0
5.5

NRL Memorandum Report 3385

Numerical Solution of the Parabolic Equation with the PEP Code

B. E. McDONALD

Plasma Dynamics Branch
Plasma Physics Division

October 1976

NAVAL RESEARCH LABORATORY
Washington, D.C.

SECURITY CLASSIFICATION OF THIS PAGE (When Data Entered)

REPORT DOCUMENTATION PAGE

READ INSTRUCTIONS BEFORE COMPLETING FORM

1. REPORT NUMBER: NRL Memorandum Report 3385
2. GOVT ACCESSION NO.
3. RECIPIENT'S CATALOG NUMBER

4. TITLE (and Subtitle): NUMERICAL SOLUTION OF THE PARABOLIC EQUATION WITH THE PEP CODE
5. TYPE OF REPORT & PERIOD COVERED: Interim report on a continuing NRL problem.
6. PERFORMING ORG. REPORT NUMBER

7. AUTHOR(s): B. E. McDonald
8. CONTRACT OR GRANT NUMBER(s)

9. PERFORMING ORGANIZATION NAME AND ADDRESS: Naval Research Laboratory, Washington, D.C. 20375
10. PROGRAM ELEMENT, PROJECT, TASK AREA & WORK UNIT NUMBERS: NRL Problem A03-16; RR033-02-42-5308

11. CONTROLLING OFFICE NAME AND ADDRESS
12. REPORT DATE: October 1976
13. NUMBER OF PAGES: 22

14. MONITORING AGENCY NAME & ADDRESS (if different from Controlling Office)
15. SECURITY CLASS. (of this report): UNCLASSIFIED
15a. DECLASSIFICATION/DOWNGRADING SCHEDULE

16. DISTRIBUTION STATEMENT (of this Report)
Approved for public release; distribution unlimited.

NRL-MR-3385

17. DISTRIBUTION STATEMENT (of the abstract entered in Block 20, if different from Report)

RR033002 RR033042

18. SUPPLEMENTARY NOTES

19. KEY WORDS (Continue on reverse side if necessary and identify by block number)
Propagation
Random media
Refraction
Parabolic equation

20. ABSTRACT (Continue on reverse side if necessary and identify by block number)
Proposed is ~~We propose~~ a centered leapfrog difference scheme for solution of the parabolic equation for wave propagation in random media. ~~We give~~ stability and resolution requirements for the scheme are given. Results of two numerical integrations are in good agreement with those obtained by others using different methods.

DD FORM 1 JAN 73 1473 EDITION OF 1 NOV 65 IS OBSOLETE
S/N 0102-014-6601

SECURITY CLASSIFICATION OF THIS PAGE (When Data Entered)

251950 AB

CONTENTS

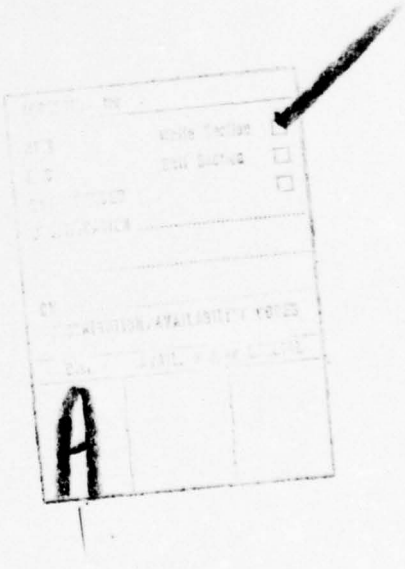

NUMERICAL SOLUTION OF THE PARABOLIC EQUATION WITH THE PEP CODE

1. THE WAVE EQUATION

We are concerned with obtaining numerical solutions to the three-dimensional wave equation

$$[\nabla^2 + k_o^2 (1 + \chi(\underset{\sim}{r}))] E(\underset{\sim}{r}) = 0 \qquad (1)$$

in a region of space where the index of refraction varies slowly with $\underset{\sim}{r}$. Subject to certain assumptions, (1) describes radio propagation through a spatially varying plasma[1], or acoustic wave propagation through a medium in which the sound speed is a function of space[2]. The solution E is assumed to have a time dependence $e^{i\omega t}$, and the wavenumber k_o is ω/c, where c is the speed of light for the radio application, or a reference sound speed for the acoustic application.

For radio wave propagation, $E(\underset{\sim}{r})$ is a scalar component of the electric field, and $\chi(\underset{\sim}{r})$ is the known electric susceptibility of the plasma. Equation (1) neglects a depolarization term whose magnitude is approximately $k_o |E\nabla\chi|$ for small χ. If χ varies on a length scale L, the depolarization term is smaller than the $k_o^2 \chi$ term of (1) by a factor $1/k_o L$. We shall be interested in applications in which $L \gg 1/k_o$, so the depolarization term is expected to be negligible. The use of a scalar χ also assumes implicitly that magnetization is unimportant; namely, that ω is much greater than the electron cyclotron frequency.

For acoustic applications, E is the sound pressure, and χ is a measure of the sound speed fluctuation such that the local sound speed

Note: Manuscript submitted September 20, 1976.

is $c/\sqrt{1 + \chi(\underset{\sim}{r})}$. Just as in the radio wave application, a term involving the gradient of χ has been neglected, but again, its magnitude is down from that of the χk_o^2 term by a factor $1/k_o L$.

For solutions of (1), let us make the substitution

$$E(\underset{\sim}{r}) = u(\underset{\sim}{r})\, e^{i\int k(z)dz} , \tag{2}$$

where

$$k(z) = k_o \sqrt{1 + \chi_o(z)} , \tag{3}$$

and $\chi_o(z)$ is some "background" χ profile along an assumed propagation direction z. The geometry of the problem is illustrated in Figure 1. For reasons of computational efficiency to be demonstrated later, (2) is in some cases preferable to a more standard approach[3,4] in which the phase factor is taken to be $e^{ik_o z}$. Substitution of (2) into (1) gives

$$\nabla^2 u + 2ik(z)\, \partial_z u + u(i\partial_z k + k_o^2\, \chi_1) = 0 \tag{4}$$

where

$$\chi_1(\underset{\sim}{r}) = \chi(\underset{\sim}{r}) - \chi_o(z) . \tag{5}$$

One further transformation is useful before introducing the parabolic approximation: let

$$f(\underset{\sim}{r}) = u(\underset{\sim}{r})\, (k/k_o)^{\frac{1}{2}} \tag{6}$$

$$= u(\underset{\sim}{r})\, (1 + \chi_o(z))^{\frac{1}{4}} .$$

Thus $$E(\underset{\sim}{r}) = f(\underset{\sim}{r})\, (1 + \chi_o(z))^{-\frac{1}{4}}\, e^{i\int k(z)dz} . \tag{7}$$

Then (4) becomes

$$\nabla_\perp^2 f + k^{\frac{1}{2}}\, \partial_z^2\, (f k^{-\frac{1}{2}}) + 2ik\partial_z f + f k_o^2 \chi_1 = 0 , \tag{8}$$

Where $\perp$ refers to the two Cartesian coordinates x and y orthogonal to z. It is important to note that no approximations have been introduced

between (1) and (8).

2. THE PARABOLIC APPROXIMATION

If we assume that f is substantially constant over a distance of one wavelength

$$\lambda = 2\pi/k_o \ , \tag{9}$$

and that $|\chi_1| \ll 1$, (10)

the second z derivative in (8) becomes negligible in comparison with the first z derivative. To define what "negligible" means, let us assume that f varies on a length scale $L \gg \lambda$ and assign constant values to k and χ_1. We Fourier transform f according to

$$f(\underset{\sim}{r}) = \int \tilde{f}(\underset{\sim}{P}) e^{i\underset{\sim}{P} \cdot \underset{\sim}{r}} \, d\underset{\sim}{P} \ . \tag{11}$$

The transform of (8) then gives

$$-P_\perp^2 - P_z^2 - 2k P_z + k_o^2 \chi_1 = 0 \ . \tag{12}$$

Because of the slow variation assumed for f, we can assign a limiting value to $P_\perp$:

$$P_\perp^2 \leq 1/L^2 \ . \tag{13}$$

If we take $k \approx k_o$, (12) and (13) give a limiting value for P_z:

$$\left(\frac{P_z}{k_o}\right)^2 + 2\,\frac{P_z}{k_o} \to \chi_1 - \frac{1}{k_o^2 L^2} \ . \tag{14}$$

The right side of (14) is small by assumption, so

$$\frac{P_z}{k_o} \to \frac{1}{2}\left(\chi_1 - \frac{1}{k_o^2 L^2}\right) + O\left(\left(\chi_1 - \frac{1}{k_o^2 L^2}\right)^2\right) \tag{15}$$

Since the quadratic term can be dropped from (14), the second z

derivative may be dropped from (8):

$$\partial_z f = \frac{i}{2k} \left(\nabla_\perp^2 f + k_o^2 \chi_1 f \right) . \qquad (16)$$

This is the "parabolic equation" for f. The fractional error in f resulting from the parabolic approximation is on the order of

$$\left| \chi_1 - \frac{1}{k_o^2 L^2} \right| .$$

3. NUMERICAL INTEGRATION OF THE PARABOLIC EQUATION

Note that (16) represents an initial value problem with regard to z integration. We can specify f at some initial z to describe an incident wave, and use (16) to step through a region of arbitrarily varying χ_1. Previous numerical application of the parabolic equation to the ionospheric scintillation problem has been primarily oriented toward propagation into <u>free space</u> of a wave which has just emerged from a random phase screen[4]. In this application, one Fourier transforms the initial f(x,y,o), advances the phase of each spectral component in an appropriate way, and then transforms back to get f(x,y,z). However, by integrating (16) <u>within</u> the scattering medium, one can follow the growth of amplitude and phase variations in an arbitrarily thick slab.

A. FINITE DIFFERENCE SCHEME

We propose a leapfrog scheme to integrate (16), with real and imaginary parts of f defined on alternate z levels (see Figure 2).

Let us express f explicitly in terms of real and imaginary parts:

$$f(\underset{\sim}{r}) = f_r(\underset{\sim}{r}) + i f_i(\underset{\sim}{r}) \tag{17}$$

where f_r and f_i are real. Then (16) gives the coupled linear system:

$$\partial_z f_r = \frac{-1}{2k}\left(\nabla_\perp^2 f_i + k_o^2 \chi_1 f_i\right) \tag{18}$$

$$\partial_z f_i = \frac{1}{2k}\left(\nabla_\perp^2 f_r + k_o^2 \chi_1 f_r\right) \quad .$$

This system may be integrated on a staggered mesh, with f_r and f_i defined on alternate z levels. The three functions f_r, f_i, and χ_1 are discretized in (x,y,z) space with integer indices (I,J,K). The mesh spacings in the x and y directions are the same value, δx; the spacing between the z planes is δz. We shall use the following second order difference formulas:

$$\partial_z f(k) \to \frac{f(k+1) - f(k-1)}{2\delta z} \tag{19}$$

$$\nabla_\perp^2 f(I,J,K) \to [f(I+1,J,K) + f(I-1,J,K) + f(I,J+1,K) + f(I,J-1,K) - 4f(I,J,K)]/\delta x^2$$

B. STABILITY ANALYSIS

If an additive error $\epsilon = \epsilon_r + i\epsilon_i$ is introduced into a discretized solution f, then ϵ itself must satisfy (18). This error may be Fourier analyzed, and stability analysis applied to each spectral component. We take χ_1 constant, set $k = k_o$ for simplicity, and take

$$\epsilon(\underset{\sim}{r}) \propto e^{i(P_x X + P_y Y + P_z Z)} \quad . \tag{20}$$

For a specific choice of (P_x, P_y, P_z), the derivative operators ∂_z and $\nabla_\perp^2$ may be treated as algebraic multipliers. Substitution of (20) into (16) gives

$$\partial_z = \frac{i}{2k_o} (\nabla_\perp^2 + k_o \chi_1), \tag{21}$$

where

$$\partial_z = \frac{e^{iP_z\delta_z} - e^{-iP_z\delta z}}{2\delta z} \tag{22}$$

$$= i\sin(P_z\delta z)/\delta z ,$$

and $$\nabla_\perp^2 = -\frac{2}{\delta x^2}[2 - \cos(P_x\delta x) - \cos(P_y\delta x)] \tag{23}$$

For investigating stability of integrating forward in the z direction, we set

$$\gamma = e^{iP_z\delta z} . \tag{24}$$

The stability criterion will be $|\gamma| \leq 1$. Now (21) gives the quadratic equation

$$\gamma - \gamma^{-1} = i\mu , \tag{25}$$

where

$$\mu = \frac{\delta z}{k_o}\left(\nabla_\perp^2 + k_o^2 \chi_1\right) . \tag{26}$$

The solution to (25) is

$$\gamma = i\frac{\mu}{2} \pm \sqrt{1 - \mu^2/4} \tag{27}$$

When $\mu^2/4 > 1$, one of the roots gives $|\gamma| > 1$, and the scheme is unstable. When $\mu^2/4 \leq 1$, the radical in (27) is real, and

$$|\gamma|^2 = \left(\frac{\mu}{2}\right)^2 + (1 - \mu^2/4) = 1. \tag{28}$$

Thus the stability criterion is

$$|\mu| \leq 2 \tag{29}$$

The greatest possible value of $|\mu|$ occurs when $\nabla_\perp^2 = -8/\delta x^2$, and

$\chi_1 < 0$. Thus all modes are stable when the following is satisfied:

STABILITY REQUIREMENT:
$$\delta z \leq \frac{2k_o}{8/\delta x^2 + k_o^2 |\chi_1|} \quad . \tag{30}$$

This criterion demonstrates the advantage of separating the background χ_o from the fluctuations χ_1. If we had used $e^{ik_o z}$ as a phase factor in (2), then χ_1 in (30) would be replaced by $\chi_o + \chi_1$. In typical applications, this would result in a smaller stepsize δz.

In addition to the stability criterion (30) we wish also to impose a resolution requirement that δ change by only a "small amount" from one z level to the next. By this we mean that the function f in (16) should undergo a phase change less than one radian over a distance $2\delta z$:

$$|2p_z \delta z| \leq 1 \ , \tag{31}$$

where the limiting form (15) is used for p_z.

Thus we have

RESOLUTION REQUIREMENT:
$$\delta z \leq k_o^{-1} \left(|\chi_1| + \frac{1}{k_o^2 L^2} \right)^{-1} \tag{32}$$

We have made changes in going to (15) to (33) to account for the fact that χ_1 may be positive or negative. The ratio of the largest δz permitted by the resolution condition to the largest value allowed by the stability condition is

$$\frac{\delta z_R}{\delta z_S} = \frac{8/\delta x^2 + k_o^2 \ |\chi_1|}{2(1/L^2 + k_o^2 \ |\chi_1|} \ , \tag{33}$$

where δz_R and δz_S are taken from (32) and (31) respectively. For small

χ_1, this ratio tends to $4L^2/\delta x^2$. This value is by assumption greater than one for all cases that can be considered within the framework of a discrete point representation. When the χ_1 term dominates, (33) tends toward the value $^1/_2$. To insure stability and adequate resolution, we take the lesser of (30) and (32) for δz. This can be summarized as follows:

When $k_o^2 |\chi_1| \leq 8/\delta x^2 - 2/L^2$ use (30)

" > " use (32).

We have treated $|\chi_1|$ as a constant in writing (30) - (33). In practice, one would use the maximum value at a given z level to determine the stepsize δz.

C. BOUNDARY CONDITIONS

In the examples to be presented in the next section we have used a very simple (although arbitrary) algorithm for defining the Laplacian operator $\nabla_\perp^2$ at the edges of the mesh. Namely, we have set the normal second derivative equal to zero at all locations one cell from the boundary. We confine the calculation to the interior mesh. Suppose that the (x,y) mesh consists of NX by NY points. Then for all J and K we impose the condition

$$f(1,J,K) = 2f(2,J,K) - f(3,J,K) \qquad (34)$$

$$f(NX,J,K) = 2f(NX-1,J,K) - f(NX-2,J,K) .$$

A straightforward extension of (34) defines f for J = 1 and NY. In practice, we use (18) and (19) to update f on the interior mesh I = 2 to NX-1, J - 2 to NY-1, and define f on the boundaries with (34). We have so far not noticed any stability or accuracy problems resulting

from (34).

D. RESULTS FROM THE PEP CODE

We have two comparisons to present between numerical solutions to (18) and published results obtained by other means. We have carried out the numerical procedure defined in (18) and (19) and included certain diagnostic features in a "Parabolic Equation Propagation" code, whose acronym is conveniently PEP. Values for the real and imaginary parts of f are assigned at some initial z level. The PEP code steps (18) forward, and at specified intervals computes "scintillation indices," phase variances in radians, and power variances in decibels. The scintillation index of greatest interest is

$$s_4(z) = \frac{\sqrt{\langle |f|^4 \rangle - \langle |f|^2 \rangle^2}}{\langle |f|^2 \rangle} \quad , \tag{35}$$

where the bracket $\langle\ \rangle$ refers to an average over x and y, with z fixed. The phase and power variances are respectively

$$\sigma_\Phi^2(z) = \langle \Phi^2 \rangle - \langle \Phi \rangle^2 \tag{36}$$

where

$$\Phi = \mathrm{Tan}^{-1}\, f_i/f_r \ ; \text{ and}$$

$$\sigma_\chi^2(z) = 100 \langle (\mathrm{Log}_{10} |f|^2)^2 \rangle - 100 \langle \mathrm{Log}_{10} |f|^2 \rangle^2 \ . \tag{37}$$

The notation conflict between the power variance σ_χ and the susceptibility χ is a result of established conventions in ionospheric and plasma physics literature.

1. Focusing by a Gaussian Lens

First we consider a wave incident on a two dimensional lens (x, z) whose thickness in terms of phase delay is

$$\Phi(x,o) = 10 \exp\ (- (x/\ell)^2) \qquad (38)$$

radians. This problem has been examined numerically by Buckley[5] using a small angle diffraction approach. Our approach is to solve the initial value problem (16) with $\chi_1 = 0$ everywhere below the lens ($z \lesssim 0$), and with initial conditions

$$f(x,o) = e^{i\Phi(x,0)} . \qquad (39)$$

The two dimensional problem was integrated according to the prescription (18) - (19) with the J index suppressed. Numerical values used for the integration were: $\delta x = .05$, $\delta z = 0.314159$, $\lambda = .01$, $\ell = 1$, NZ = 402, and NX = 82. Results for the "power" $|E(x,z)|^2 = |f(x,z)|^2$ are in Figure 3. The qualitative agreement with Buckley's result[5] is quite satisfactory. Z in Figure 3 is a dimensionless coordinate which can be used to scale equation (16):

$$Z = z/k\ell^2 \qquad (40)$$

2. Diffraction from a Random Phase Screen

Let us consider a three dimensional problem in which the initial phase $\Phi(x,y,o)$ is a random function of x and y with Gaussian autocorrelation:

$$\langle \Phi(x,y,o)\ \Phi(x+\xi, y+\eta, 0) \rangle = \Phi_o^2 e^{-(\xi^2+\eta^2)/r_o^2} . \qquad (41)$$

Such a function can be generated numerically by Fourier transforming the desired spatial autocorrelation function, multiplying each Fourier

component by a random phase factor $e^{i\varpi}$, and then transforming back into xy space. In this prescription, ϖ is an arbitrarily generated number ranging from 0 to 2π. To insure that ϕ is real, one can assign ϖ arbitrarily in one half of the transform space (k_x, k_y) and then set $\varpi(-k_x, -k_y) = -\varpi(k_x, k_y)$.

We have generated a function satisfying (41) to use as an initial condition for (16). We initialize the calculation with

$$f(x,y,o) = e^{i\phi(x,y,o)} \tag{42}$$

and integrate forward into free space ($x = 0$). Four curves showing computed values of S_4 versus propagation distance for different values of ϕ_o appear in Figure 4. The dots are from the calculation, and the solid curves are the results of Mercier[6] plotted in the format of Briggs and Parkin[7]. The results are in good agreement with the solid curves. The data used to generate these results were $\delta x = .002$, $\delta z = .015$, $\lambda = .0001$, $r_o = .01$, NX = 27, NY = 27, and NZ = 102.

SUMMARY

We have described a set of coupled linear equations (18) which result from the wave equation (1) in the parabolic approximation. Equations (18) differ from the usual "parabolic equation" only in that the index of refraction is allowed to vary slightly along an assumed propagation direction as part of the background or unscattered state. A rough estimate of the error introduced by the parabolic approximation is given after (16). We have constructed the PEP code for finite difference solution of (18) using the centered leapfrog scheme (19). The stability criterion for the scheme is (30).

Results from the PEP code are in good agreement with those obtained by different means for refraction due to a Gaussian lens and for refraction due to a random phase screen. These two examples involve propagation into a vacuum of an initially specified wave. Results for propagation within a scattering medium will be given elsewhere.

REFERENCES

1. K. C. Yeh and C. H. Liu, Theory of Ionospheric Waves (Academic Press, New York, 1972), Chap. 6
2. P. M. Morse, Theoretical Acoustics (McGraw Hill, New York, 1968), Equation 8.1.12.
3. Y. N. Barabanenkov, Y. A. Kravtsov, S. M. Rytov and V. I. Tatarskii, Soviet Phys. Uspekhi (English translation) 13, 551, 1971.
4. R. H. Hardin and F. D. Tappert, "Analysis, Simulation, and Models of Ionospheric Scintillation," Bell Laboratories Report, March 1, 1974.
5. R. Buckley, J. Atmos. Terr. Phys. 37, 1431, 1975.
6. R. P. Mercier, Proc. Camb. Phil. Soc. 58, 382, 1962.
7. B. H. Briggs and I. A. Parkin, J. Atmos. Terr. Phys. 25, 339, 1963.

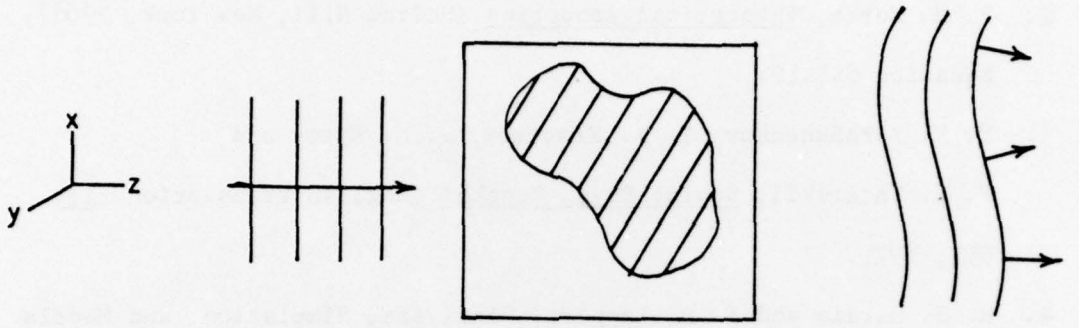

Fig. 1 — A wave incident along the z direction is scattered by inhomogeneities in the scattering volume

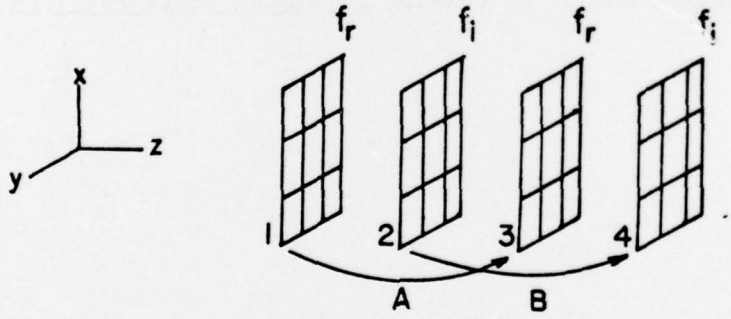

Fig. 2 — Leapfrog difference scheme. Step A updates the real part of f from plane 1 to plane 3 according to (18) and (19). Then Step B updates the imaginary part of f from plane 2 to plane 4.

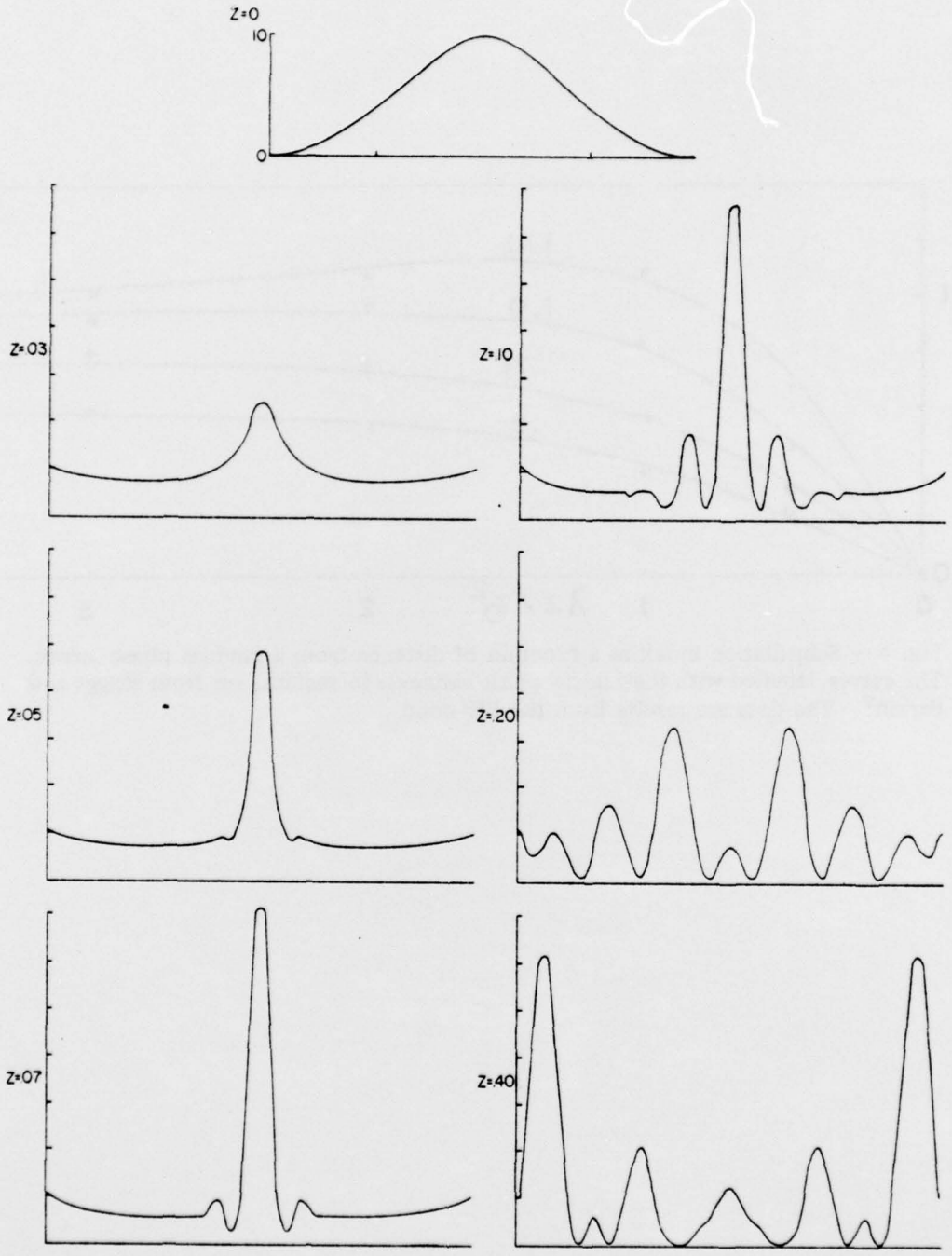

Fig. 3 — Diffraction due to a Gaussian lens. At the top is phase delay in radians for Z = 0. The other curves are the power, $|f|^2$, at distances Z (see (40)) from the lens.

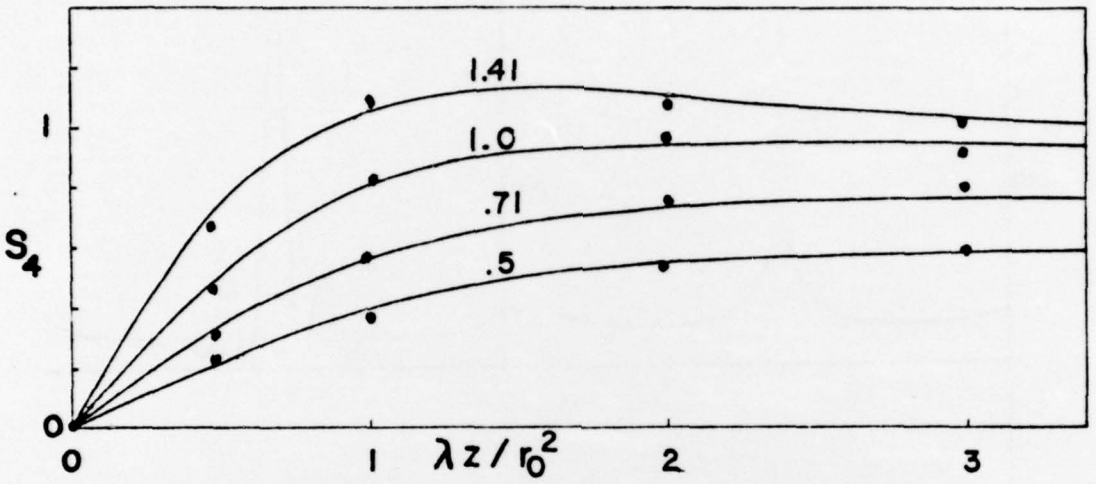

Fig. 4 — Scintillation index as a function of distance from a random phase screen. The curves, labelled with their initial phase variances in radians, are from Briggs and Parkin[7]. The dots are results from the PIP code.

DISTRIBUTION LIST

Advanced Research Projects Agency (ARPA)
Strategic Technology Office
Arlington, Virginia

Capt. Donald M. LeVine

Naval Research Laboratory
Washington, D. C. 20375

Dr. P. Mange
Dr. E. Peterkin
Dr. R. Meier
Dr. E. Szuszczewicz -- Code 7127
Dr. Timothy Coffey -- Code 7700 (20 copies)
Dr. J. Goodman -- Code 7950

Science Applications, Inc.
1250 Prospect Plaza
La Jolla, California 92037

Dr. D. A. Hamlin
Dr. L. Linson
Dr. D. Sachs

Director of Space and Environmental Laboratory
NOAA
Boulder, Colorado 80302

Dr. A. Glenn Jean
Dr. G. W. Adams
Dr. D. N. Anderson
Dr. K. Davies
Dr. R. F. Donnelly

A. F. Cambridge Research Laboratories
L. G. Hanscom Field
Bedford, Mass. 01730

Dr. T. Elkins
Dr. W. Swider
Mrs. R. Sagalyn
Dr. J. M. Forbes
Dr. T. J. Keneshea
Dr. J. Aarons

Office of Naval Research
800 North Quincy Street
Arlington, Virginia 22217

Dr. J. G. Dardis
Dr. H. Mullaney

Commander
Naval Electronics Laboratory Center
San Diego, California 92152

Dr. M. Bleiweiss
Dr. I. Rothmuller
Dr. V. Hildebrand
Mr. R. Rose

U. S. Army Aberdeen Research and Development Center
Ballistic Research Laboratory
Aberdeen, Maryland

Dr. F. Niles
Dr. J. Heimerl

Commander
Naval Air Systems Command
Department of the Navy
Washington, D. C. 20360

Dr. T. Czuba

Harvard University
Harvard Square
Cambridge, Mass.

Dr. M. B. McElroy
Dr. R. Lindzen

Pennsylvania State University
University Park, Pennsylvania 16802

Dr. J. S. Nisbet
Dr. P. R. Rohrbaugh
Dr. D. E. Baran
Dr. L. A. Carpenter
Dr. M. Lee
Dr. R. Divany
Dr. P. Bennett
Dr. E. Klevans

University of California, Los Angeles
405 Hillgard Avenue
La Jolla, California 90024

Dr. F. V. Coroniti
Dr. C. Kennel

University of California, San Diego
P. O. Box 109
La Jolla, California 92037

Dr. P. M. Banks

Utah State University
4th N. and 8th E. Streets
Logan, Utah 84322

Dr. R. Harris
Dr. V. Peterson
Dr. R. Megill

Cornell University
Ithaca, New York 14850

Dr. W. E. Swartz
Dr. R. Sudan
Dr. D. Farley
Dr. M. Kelley

NASA
Goddard Space Flight Center
Greenbelt, Maryland 20771

Dr. S. Chandra
Dr. K. Maedo

Princeton University
Plasma Physics Laboratory
Princeton, New Jersey 08540

Dr. F. Perkins

Institute for Defense Analysis
400 Army/Navy Drive
Arlington, Virginia 22202

Dr. E. Bauer